The Astrophysical Journal, 631:488–494, 2005 September 20

MAGNETOSPHERIC ECLIPSES IN THE DOUBLE-PULSAR SYSTEM PSR J0737−3039

Roman R. Rafikov[1] and Peter Goldreich[1,2]
Received 2005 January 13; accepted 2005 May 23

ABSTRACT

We argue that eclipses of radio emission from the millisecond pulsar A in the double-pulsar system PSR J0737−3039 are due to synchrotron absorption by plasma in the closed field line region of the magnetosphere of its normal pulsar companion B. On the basis of a plausible geometric model, pulsar A's radio beam only illuminates pulsar B's magnetosphere for about 10 minutes surrounding the time of eclipse. During this time it heats particles at $r \gtrsim 10^9$ cm to relativistic energies and enables extra plasma, beyond that needed to maintain the corotation electric field, to be trapped by magnetic mirroring. An enhancement of the plasma density by a factor of $\sim 10^2$ is required to match the duration and optical depth of the observed eclipses. The extra plasma might be supplied by a source near B through $B\gamma$ pair creation by energetic photons produced in B's outer gap. Relativistic pairs cool by synchrotron radiation close to where they are born. Reexcitation of their gyrational motions by cyclotron absorption of A's radio beam can result in their becoming trapped between conjugate mirror points in B's magnetosphere. Because the trapping efficiency decreases with increasing optical depth, the plasma density enhancement saturates even under steady state illumination. The result is an eclipse with finite, frequency-dependent optical depth. After illumination by A's radio beam ceases, the trapped particles cool and are lost. The entire cycle repeats every orbital period. We speculate that the asymmetries between eclipse ingress and egress result in part from the magnetosphere's evolution toward a steady state when illuminated by A's radio beam. We predict that A's linear polarization varies with both eclipse phase and B's rotational phase.

Subject headings: plasmas — pulsars: general — pulsars: individual (PSR J0737−3039A, PSR J0737−3039B) — radiation mechanisms: nonthermal — stars: neutron

1. INTRODUCTION

The binary pulsar PSR J0737−3039—a millisecond pulsar (pulsar A with a period $P_A = 23$ ms) and a normal pulsar (pulsar B with a period $P_B = 2.8$ s) in a tight 2.4 hr orbit (Burgay et al. 2003)—not only provides us with unprecedented tests of general relativity (Lyne et al. 2004) but also reveals a variety of magnetospheric phenomena. Among the latter are variations of pulsar B's radio emission correlated with binary orbital phase (Lyne et al. 2004; Ransom et al. 2005) and modulated at the spin frequency of pulsar A (McLaughlin et al. 2004a) and periodic eclipses of pulsar A when it passes behind pulsar B (Lyne et al. 2004; Kaspi et al. 2004; McLaughlin et al. 2004b). It is the latter phenomenon that concerns us in this paper.

Detailed observations with the Green Bank Telescope (Kaspi et al. 2004) established the following frequency-averaged properties of pulsar A's eclipses: the eclipse duration is about 27 s, which for a relative transverse velocity of 680 km s^{-1} translates into a size of 18,000 km. Eclipses are significantly asymmetric, with ingress taking 3–4 times longer than egress; pulsar A's radio beam is extinguished more strongly after conjunction, consistent with zero flux, than before conjunction, when some flux leaks through. Analysis of the same data at higher time resolution by McLaughlin et al. (2004b) uncovered effects of B's rotational phase on the frequency dependence and shape of the eclipse during ingress; its shape during egress is remarkably independent of both B's rotational phase and radio frequency.

The spin-down luminosity of pulsar A exceeds that of pulsar B by a factor of $\sim$3600, so it is plausible that B's magnetosphere is compressed by a relativistic wind from A. Calculations by Lyutikov (2004) demonstrate that the ram pressure of A's wind can be balanced by B's magnetic field pressure at a standoff distance $r_{\rm so} \approx (3.5-6)\times 10^9$ cm, which is within B's light cylinder radius of $r_{L,B} \equiv c/\Omega_B \approx 1.3\times 10^{10}$ cm. A crucial point is that the size of the eclipsing region is considerably smaller than even the compressed size of B's magnetosphere. To fully quantify the geometry of the eclipse, the inclination of the system must be accurately known. Measurements of the Shapiro delay established that the inclination is very high, $i = 87^\circ \pm 3^\circ$ (Lyne et al. 2004). A refined estimate by Coles et al. (2005) based on correlation of interstellar scintillations of both pulsars yields $i = 90\overset{\circ}{.}26 \pm 0\overset{\circ}{.}13$, which corresponds to a minimum distance of A's radio beam with respect to B's position projected on the plane of the sky of only 4000 ± 2000 km. This refinement implies that the extinction during eclipse arises *inside* pulsar B's magnetosphere and that the radial extent of the eclipsing region is about 10,000 km.

Our goal is to evaluate the absorption of the radio beam of pulsar A as it passes through the magnetosphere of pulsar B. We show in § 2 that resonant cyclotron absorption in the charge-separated, closed field line region would provide only a small optical depth. However, we demonstrate in § 3 that absorption of radiation from pulsar A heats charged particles in B's magnetosphere to relativistic energies. In § 4 we describe how this enables the accumulation of additional, charge-neutral plasma in B's magnetosphere. As a result, the radio emission of pulsar A can be significantly extinguished by synchrotron absorption. We devote § 7 to a discussion of the ramifications of our model.

[1] Institute for Advanced Study, Einstein Drive, Princeton, NJ 08540; rrr@ias.edu.
[2] Theoretical Astrophysics, California Institute of Technology, MS 130-33, Pasadena, CA 91125; pmg@ias.edu.

2. RESONANT CYCLOTRON ABSORPTION

The region of closed field lines in the conventional pulsar magnetosphere model contains a corotating, charge-separated plasma with number density

$$n_{\rm GJ}(\boldsymbol{r}) = \frac{|\boldsymbol{\Omega}_B \cdot \boldsymbol{B}(\boldsymbol{r})|}{2\pi ec(1 - v^2/c^2)}, \tag{1}$$

where v is the corotation velocity (Goldreich & Julian 1969). We are primarily interested in the region of pulsar B's magnetosphere where $v \ll c$ and the magnetic field is approximately dipolar. For our simplified model it suffices to ignore the angular dependence of the field and set

$$B(r) \approx B_\star \left(\frac{R_\star}{r}\right)^3,$$
$$\boldsymbol{\Omega}_B \cdot \boldsymbol{B}(\boldsymbol{r}) \approx \Omega_B B(r), \tag{2}$$

where $R_\star$ is the neutron star radius and $B_\star$ is its surface magnetic field.

The particle *number* density n can be higher than $n_{\rm GJ}$ because the addition of neutral plasma does not affect the net charge density. We characterize this increase by the parameter $\lambda \geq 1$ defined such that

$$n(r) \approx \lambda(r) \frac{\Omega_B B(r)}{2\pi ec}. \tag{3}$$

In what follows, we assume that the magnetospheric particles are electrons and positrons.

Resonant cyclotron absorption is the dominant source of extinction for radio waves passing through a conventional pulsar magnetosphere. Cyclotron resonance occurs where

$$\omega \approx \omega_B \equiv \frac{eB}{m_e c} \tag{4}$$

with cross section (Canuto et al. 1971; Daugherty & Ventura 1978)

$$\sigma(\omega) \approx \sigma_{\rm T} \frac{\omega^2}{(\omega - \omega_B)^2 + \Gamma^2/4}, \tag{5}$$

where $\sigma_{\rm T}$ is the Thompson cross section and

$$\Gamma \equiv \frac{4e^2\omega_B^2}{3m_e c^3} \tag{6}$$

is the natural line width. Strictly speaking, this cross section applies to photons in particular modes that differ for electrons and positrons, but we ignore this detail here.

The peak cross section at resonance reaches $\sigma_{\rm max} \approx 6\pi(c/\omega_B)^2$, or roughly the square of the photon wavelength. Nevertheless, the optical depth is modest because an incident photon only resonates with cold electrons in a narrow radius range. From equations (2)–(6) we find that resonance occurs at a radial distance from pulsar B of

$$r_r(w) \approx R_\star \left(\frac{eB_\star}{m_e c}\omega^{-1}\right)^{1/3} = R_\star \left(\frac{\omega_{B\star}}{\omega}\right)^{1/3}$$
$$\approx 1400 R_\star B_{\star 12}^{1/3} \nu_9^{-1/3} \tag{7}$$

and that the optical depth is given by

$$\tau_c \approx \frac{2\pi}{3}\lambda(r_r)\frac{\Omega_B r_r}{c} \approx 0.2\lambda(r_r) B_{\star 12}^{1/3} \nu_9^{-1/3}, \tag{8}$$

where ν_9 is the radio frequency $\nu = \omega/(2\pi)$ expressed in GHz and $\omega_{B\star} = 1.8\times10^{19} B_{\star,12}$ s^{-1} is the cyclotron frequency at the surface of pulsar B (i.e., for $B = B_\star$) with $B_{\star 12} \equiv B/(10^{12}$ G). Throughout the paper we set the neutron star radius to be 10 km and use $R_\star$ as a unit of distance. Note that for the $\lambda = 1$, τ_c is approximately the ratio of the resonance radius r_r to the radius of B's light cylinder, c/Ω_B, a result obtained previously by Blandford & Scharlemann (1976) and Mikhailovskii et al. (1982).

The determination of the inclination of the binary's orbit to the plane of the sky based on the scintillation technique (Coles et al. 2005) implies that the radio beam of pulsar A passes pulsar B at an impact parameter $p \sim 4\times10^8$ cm. Since $p \lesssim r_r$, at a first glance cyclotron absorption looks like a viable eclipse mechanism, although a $\lambda \sim 10$–100 would be required to match the eclipse depth. However, a closer look at cyclotron absorption, as described below, reveals a problem: A's radio radiation heats the particles in B's magnetosphere to relativistic energies, making synchrotron absorption rather than cyclotron absorption the relevant process.

We denote by $F_\omega(\omega, r)$ the energy flux per unit frequency from pulsar A at distance r from pulsar B. A nonrelativistic electron or positron absorbs and emits energy, respectively, at the rate (Rybicki & Lightman 1979)

$$\dot{E}_+(r) = \frac{1}{2}\int F_\omega(\omega, r)\sigma(\omega)\, d\omega$$
$$= 2\pi^2 \frac{e^2}{m_e c} F_\omega(\omega_B(r), r), \tag{9}$$

$$\dot{E}_-(r) = \frac{4}{9}\frac{e^4}{m_e^2 c^3}(\beta\gamma)^2 B(r)^2, \tag{10}$$

where $\gamma \equiv (1 - \beta^2)^{1/2}$ is the Lorentz factor of the electrons and positrons, which must be close to unity for cyclotron absorption and emission to pertain. Balancing $\dot{E}_+$ by $\dot{E}_-$ yields

$$\beta\gamma = \frac{3\pi}{2}\left[\frac{F_\omega(\omega_B(r)r, r)}{\omega_B^2 m_e}\right]^{1/2}. \tag{11}$$

Lyne et al. (2004) measure a time-averaged flux density of $\approx$1.6 mJy at $\nu_0 \equiv \omega_0/(2\pi) = 1.4$ GHz from pulsar A. Taking 600 pc for the distance to PSR J0737−3039, one obtains $F_0 \equiv F_\omega(\omega_0) \approx 10^{-6}$ ergs cm^{-2} at the position of B, which is separated from A by about 9×10^{10} cm. Using equation (11), we find that at $r_r \approx 1250 R_\star B_{\star 12}$, where 1.4 GHz photons get absorbed, the electrons and positrons have $\beta\gamma \approx 25$. This means that the electrons and positrons are relativistic and that the cyclotron approximation is inapplicable. The timescale for particles to become mildly relativistic ($E \sim m_e c^2$) due to cyclotron absorption is

$$t_{\rm heat}^c(r) \approx \frac{m_e c^2}{\dot{E}_+(r)} = \frac{m_e^2 c^3/e^2}{2\pi^2 F_\omega(\omega_B(r), r)}, \tag{12}$$

which is about 5 s at the position where 1.4 GHz photons are resonantly absorbed.

A related example of the heating of particles to relativistic energies through resonant cyclotron absorption of radio waves is given in Lyubarskii & Petrova (1998). In their example the pulsar's radio waves heat particles streaming along its open field lines.

3. SYNCHROTRON ABSORPTION

The mean cross section for synchrotron absorption by an isotropic distribution of particles with energy $\gamma m_e c^2$ is (Rybicki & Lightman 1979)

$$\sigma_s(\omega) \approx \frac{8\pi^2}{3^{4/3}\Gamma(1/3)} \frac{e}{B} \left(\frac{\omega_B}{\gamma\omega}\right)^{5/3}, \quad (13)$$

provided $\omega_B/\gamma \lesssim \omega \lesssim \gamma^2\omega_B$. Here $\Gamma(x)$ is a complete gamma function.

In the absence of published measurements of pulsar A's radio spectrum, we assume that it is a power law with most of the energy concentrated at low frequencies (i.e., $F_\omega \propto \omega^{-\delta}$ with $\delta > 1$), as is typical for millisecond pulsars (Kuzmin & Losovsky 2001). The position of the low-frequency cutoff of the spectrum is not very important for our problem (however, see § 6).

For the cross section (eq. [13]) and an incident spectrum with $\delta > 1$, particle heating is dominated by the lowest frequencies. This also implies that A's radio beam suffers a low-frequency cutoff that progresses toward higher frequency with increasing depth in B's magnetosphere. Consequently, the absorbed spectrum of A's radio flux at distance r from pulsar B takes the form

$$F_\omega(\omega, r) = F_0 \left(\frac{\omega_0}{\omega}\right)^\delta \exp(-\tau_\omega(\omega, r)), \quad (14)$$

where $\tau_\omega(\omega, r)$ is the frequency-dependent optical depth at r. Using equations (3) and (13) one finds

$$\tau_\omega(\omega, r) = \int_r^\infty \sigma_s(\omega) n(r)\, dr \approx \frac{4\pi}{3^{4/3}\Gamma(1/3)\zeta_1} \lambda(r) \frac{\Omega_B r}{c} \left(\frac{\omega_B}{\gamma\omega}\right)^{5/3}, \quad (15)$$

where in arriving at the last expression we have assumed that $\lambda(r)(\omega_B/\gamma)^{5/3}$ is a steeply decreasing function of r and

$$\zeta_1 = 4 + \frac{5}{3}\frac{d\ln\gamma}{d\ln r} - \frac{d\ln\lambda}{d\ln r}. \quad (16)$$

Expression (15) is valid provided $\omega \gtrsim \omega_B/\gamma$; below this frequency the relativistic plasma becomes transparent. Since extinction at observed frequencies occurs at $r \sim 10^9$ cm $\ll r_{L,B} = c/\Omega_B \approx 10^{10}$ cm, a large $\lambda(r)$ is required to account for $\tau_\omega \gtrsim 1$.

Next, we give a simplified evaluation of the energies to which magnetospheric particles are heated, assuming that $\delta = 2$ and that λ is independent of r.[3] We define a local cutoff frequency $\omega_1(r)$ such that $\tau_\omega(\omega_1(r), r) = 1$. Using equation (15) and dropping constant coefficients, we find

$$\omega_1(r) \approx \frac{\omega_B(r)}{\gamma(r)} \left[\lambda(r)\frac{\Omega_B r}{c}\right]^{3/5}. \quad (17)$$

Clearly, $\omega_1(r)$ increases as r decreases. Figure 1 illustrates how the low-frequency part of $F_\omega(\omega, r)$ erodes with increasing depth in B's magnetosphere.[4] The synchrotron heating rate, $\dot{E}^s_+$, is given by

$$\dot{E}^s_+(r) \approx \sigma(\omega_1(r))\omega_1(r) F_\omega(\omega_1(r), r) \approx F_0 \left(\frac{\gamma\omega_0}{\omega_B}\right)^2 \frac{e}{B}\frac{\omega_B}{\gamma}\left[\lambda(r)\frac{\Omega_B r}{c}\right]^{-8/5}, \quad (18)$$

[3] Appendix A contains a more detailed derivation suitable for an arbitrary value of δ.

[4] The low-frequency cutoff of A's spectrum is unimportant inside the radius at which the cutoff frequency falls below $\omega_1(r)$.

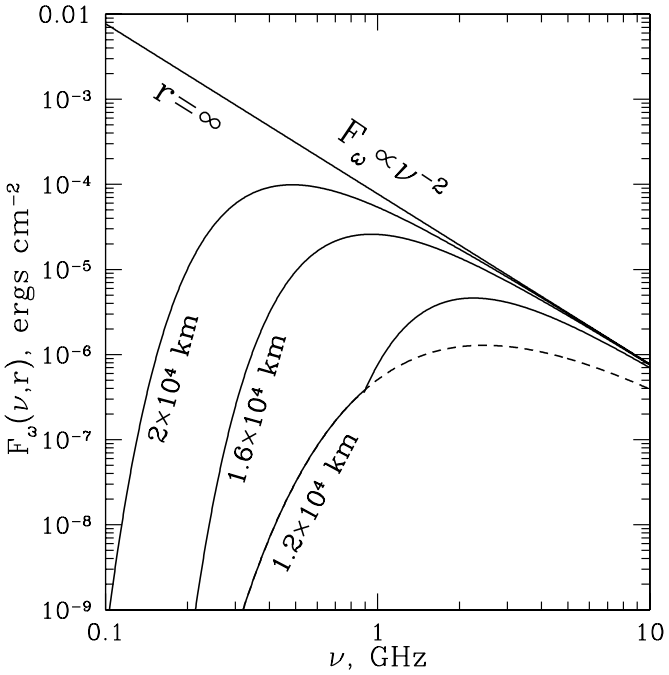

FIG. 1.—Evolution of pulsar A's radio spectrum due to synchrotron absorption in pulsar B's steady state magnetosphere, assuming $\chi = 2$. The solid curves are labeled by their distances from B. The dashed curve illustrates the maximally absorbed [with optical depth equal to $\tau_{\max}(\nu)$; see eq. (32)] spectrum close to B.

which reflects the dominance of radiation with $\omega \sim \omega_1(r)$. Balancing the synchrotron heating rate by the synchrotron cooling rate (eq. (10]) we obtain

$$\gamma(r) \approx 5\times10^2 \frac{F_0}{m_e\omega^2_{B\star}} \left(\frac{\omega_0}{\omega_{B\star}}\right)^2 \times \left(\lambda\frac{\Omega_B R_\star}{c}\right)^{-8/5} \left(\frac{r}{R_\star}\right)^{52/5} \approx 2.5\times10^4 \lambda^{-8/5} \left(\frac{r/R_\star}{10^3}\right)^{52/5} B^{-4}_{\star12} \quad (19)$$

(constant coefficients appearing in eqs. [19] and [20] are derived in Appendix A). The calculation of $\gamma(r)$ tacitly assumes that synchrotron absorption of A's radio emission is the only source for heating particles in B's magnetosphere (for a different view, see Lyutikov & Thompson 2005).

To evaluate the size of the eclipsing region $r_e(\omega)$, defined as the distance from pulsar B at which $\tau_\omega(\omega, r_e) = 1$, we combine equations (17) and (19) to arrive at

$$r_e(\omega) = 0.54 R_\star \left(\frac{\omega_{B\star}}{\omega}\right)^{5/64} \times \left[\frac{F_0}{m_e\omega^2_{B\star}}\left(\frac{\omega_0}{\omega_{B\star}}\right)^2\right]^{-5/64} \left(\lambda\frac{\Omega_B R_\star}{c}\right)^{11/64} \approx 380 R_\star \lambda^{11/64} \nu_9^{-5/64} B^{25/64}_{\star12}. \quad (20)$$

The weak frequency dependence of r_e is an artifact of the assumed constancy of λ.

The observed eclipse duration corresponds to $r_e \approx 10^9$ cm at $\nu = 1$ GHz. From equation (20) we find that this implies

$\lambda \approx 270$. For this value of λ, equation (19) yields $\gamma \approx 3.2\ B_{\star 12}^{-4}$ at $r_e = 10^9$ cm, so our assumption of synchrotron absorption is marginally valid. The optical depth τ_ω cannot be arbitrarily high, because radio photons of frequency ω are not absorbed within the radius at which $\omega \approx \omega_B/\gamma = \omega$. This "saturation" of τ_ω can be used to probe the dependence of λ on r (see eq. [32] for a particular example).

4. ENHANCEMENT OF PARTICLE NUMBER DENSITY IN THE MAGNETOSPHERE OF PULSAR B

We hypothesize that there is a continuous supply of energetic particles within the closed field line region of pulsar B's magnetosphere from a source located close to the star where the magnetic field is strong. Radiation damps the gyrational motions of particles born in this region before they can slide out along magnetic field lines. Under normal circumstances each particle would loop along the closed field line on which it was born and strike the star's surface in the opposite magnetic hemisphere. However, illumination by pulsar A's radio beam can reexcite the gyrational motions of particles that stream far away from pulsar B and then keep them suspended between conjugate mirror points (see § 4.2). Thus, both particle heating, which makes synchrotron absorption possible, and particle trapping, which leads to a higher optical depth eclipse, are mediated by A's radio beam.

4.1. *Lifetimes of Energetic Particles*

After illumination by pulsar A's radio beam ceases, particles trapped by magnetic mirroring in pulsar B's magnetosphere cool and are lost. Synchrotron emission reduces their energies to $m_e c^2$ on a timescale $t_{\rm cool}$, independent of their initial $\gamma \gg 1$. From equation (A2), we estimate

$$t_{\rm cool} \sim \frac{m_e^3 c^5}{e^4 B^2} \approx 350\ {\rm s} \left(\frac{r/R_\star}{10^3}\right)^6 B_{\star 12}^{-2}. \tag{21}$$

At this stage, as a consequence of relativistic beaming, components of momentum parallel and perpendicular to $\boldsymbol{B}$ decay at the same rate. Subsequently, in the nonrelativistic regime, velocity components perpendicular to $\boldsymbol{B}$ decay exponentially on a timescale $t_{\rm cool}$, while those parallel to $\boldsymbol{B}$ remain nearly constant. As a result, the trapped particles sediment onto the neutron star's surface on a timescale $t_{\rm cool}$, leaving only the minimum number density of particles, $n_{\rm GJ}$, needed to support the corotation electric field. Since $t_{\rm cool}$ is much shorter than the orbital period of the double pulsar, the magnetosphere of pulsar B has to refill each time the radio beam of pulsar A illuminates it.

4.2. *Trapping of Particles by Pulsar A's Beam*

The particle cooling time, $t_{\rm cool}$, given by equation (21) is comparable to the local travel time, $\sim r/(\beta_\parallel c)$, at the distance

$$r_{\rm cool} \approx 160 R_\star \beta_\parallel^{-1/5} B_{\star 12}^{2/5} \tag{22}$$

from pulsar B. Without heating, a particle arriving at an equatorial radius r_e from a source located below $r_{\rm cool}$ would be in its lowest gyrational state. To become trapped, it has to gain enough perpendicular momentum during its outer magnetosphere passage to mirror above $r_{\rm cool}$ because of adiabatic invariant conservation.[5]

[5] The expression for the residence time, $\sim r/(\beta_\parallel c)$, and that for $r_{\rm cool}$ given by equation (22) hold in both relativistic ($\beta_\parallel \approx 1$) and nonrelativistic ($\beta_\parallel \ll 1$) regimes.

The minimum gain in $p_\perp^2$ required for trapping is

$$\Delta p_{\perp \rm min}^2 \gtrsim \left(\beta_\parallel \gamma\right)^2 (m_e c)^2 \left(\frac{r_{\rm cool}}{r_e}\right)^3, \tag{23}$$

where $\beta_\parallel$ is evaluated at r_e. So the minimum energy, $\Delta E_{\rm min}$, that a particle has to absorb at $r \sim r_e$ is

$$\Delta E_{\rm min} \gtrsim \frac{\beta_\parallel^2 \gamma}{2} m_e c^2 \left(\frac{r_{\rm cool}}{r_e}\right)^3 \approx 2 \times 10^{-3} \beta_\parallel^{7/5} \gamma m_e c^2 B_{\star 12}^{6/5} \left(\frac{r_e/R_\star}{10^3}\right)^{-3}. \tag{24}$$

Cyclotron absorption of A's unattenuated radio beam in a single passage of r_e results in an energy increase

$$\Delta E_+ \sim \int^{r_e} \dot{E}_+(r) \frac{dr}{\beta_\parallel c} \approx 2.3 \times 10^{-4} \frac{m_e c^2}{\beta_\parallel} \left(\frac{r_e/R_\star}{10^3}\right)^7, \tag{25}$$

where the last line is evaluated for $\delta = 2$. Use of the cyclotron absorption formula (9) is appropriate because the majority of particles streaming past r_e from a source interior to $r_{\rm cool}$ are at most mildly relativistic (see § 4.3).

Comparing $\Delta E_{\rm min}$ with ΔE_+, we find that trapping via cyclotron absorption and subsequent mirroring is possible for particles with

$$\beta_\parallel^{12/5} \gamma \lesssim 0.12 B_{\star 12}^{-6/5} \left(\frac{r_e/R_\star}{10^3}\right)^{10}. \tag{26}$$

Thus, particles reaching $r_e \approx 10^9$ cm with $\beta_\parallel \lesssim 0.4$ can be trapped. This threshold is not very restrictive (see § 4.3), so the rate at which λ can grow is primarily determined by the rate at which particles are injected by the source near B's surface.[6]

4.3. *Source of Particles*

We can only speculate about possible sources of particles in the corotating magnetosphere of pulsar B. The requirement that B's magnetosphere fill with an appropriate density of plasma while it is illuminated by A's radio beam is not demanding. The total number of particles needed to provide the corotating charge density in B's magnetosphere is $N_{\rm min} \sim (\Omega_B B_\star R_\star^3/ec) \ln (r_{\rm so}/R_\star) \sim 10^{30}$. Boosting this number by a factor of $\sim 10^2$ in 10^3 s implies a trapping rate $\dot{N} \sim 10^{29}\ {\rm s}^{-1}$. If every trapped particle were born with the energy $f_1 m_e c^2$ (subsequently lost as synchrotron radiation) and only a fraction $f_2 < 1$ of them were trapped, the source power would be $P \sim 10^{23} f_1/f_2$ ergs s^{-1}. For $f_1 = 10$ and $f_2 = 0.1$, this amounts to $\sim 10^{25}$ ergs s^{-1}, much smaller than the spin-down luminosity, $\sim 10^{30}$ ergs s^{-1}, estimated for pulsar B by Lyne et al. (2004).

Our favored source is the creation of $e^- e^+$ pairs on closed field lines by gamma rays with energies ~ 100 MeV emitted by particles accelerated in the outer gap of pulsar B (Cheng et al. 1986a, 1986b; Wang et al. 1998).[7] Photons from the outer gap can enter the corotating magnetosphere and propagate at

[6] The two-stream instability might in principle assist in the trapping of particles, but an unrealistically high number density is required for its growth time to be comparable to the particle residence time in the magnetosphere.

[7] We are grateful to Jonathan Arons for drawing our attention to this possibility.

significant angles to magnetic field lines. This facilitates $B\gamma$ pair creation close to the neutron star's surface. The ability of an old pulsar to maintain an active outer gap decreases as its period increases. The critical period, however, depends on the angle between the pulsar's spin and magnetic axes (Zhang et al. 2004). For the large value of this angle for pulsar B, $\sim 75^\circ$ as inferred by Lyutikov & Thompson (2005), it is plausible that the outer gap remains active.

Pairs born relativistic initially lose energy through synchrotron radiation on a timescale $\Gamma^{-1} \sim (10^{-12}\ \mathrm{s}) B_{10}^{-2}$ (see eq. [6]). As a consequence of relativistic beaming, their pitch angles remain constant until they become transrelativistic. Subsequent cooling by gyrosynchrotron radiation completely damps gyrational motions but preserves the component of velocity parallel to the magnetic field. Thus, particles streaming away from the neutron star have $\beta_\parallel \lesssim 1$. As we discussed in § 4.2, this allows for their efficient trapping when they are illuminated by A's radio beam.

5. STEADY STATE MAGNETOSPHERE

Under constant illumination by pulsar A's radio beam, pulsar B's magnetosphere would achieve a steady state. We have already described how particle energies would be set by a balance between the absorption and emission of radiation. Here we concentrate on how the particle enhancement factor λ would be fixed in the context of the discussion in § 4.

The efficiency of particle trapping drops sharply as the optical depth at the local cyclotron frequency, $\tau_\omega(\omega_B(r), r)$, increases above unity. The energy that fresh particles acquire by cyclotron absorption in passing through the magnetosphere is reduced by a factor of $\exp(-\tau_\omega(\omega_B(r), r))$ compared to ΔE_+ (see eq. [25]). Thus, increasing $\tau_\omega(\omega_B(r), r)$ lowers the maximum $\beta_\parallel$ at which particle trapping can occur (see § 4.2). The exponential dependence of trapping on optical depth suggests that $\tau_\omega(\omega_B, r)$ does not greatly exceed unity and also that it depends at most logarithmically on r. We set

$$\tau_\omega(\omega_B, r) = \chi, \tag{27}$$

where χ is a parameter that we treat as independent of r and whose precise value depends on the rate at which trapped particles are lost by unspecified relaxation processes.

For $\omega > \omega_B/\gamma$ we find using equation (15) that $\tau_\omega(\omega, r) = \tau_\omega(\omega_B, r)(\omega_B/\omega)^{5/3}$. Thus, in the steady state magnetosphere photons of frequency ω are absorbed at distance $r_e(\omega)$ such that $\omega_B(r_e) = \omega\chi^{-3/5}$. This gives

$$r_e(\omega) = \chi^{1/5} r_r(\omega) = R_\star \chi^{1/5} \left(\frac{\omega_{B\star}}{\omega}\right)^{1/3} \approx 1400 R_\star \chi^{1/5} B_{\star 12}^{1/3} \nu_9^{-1/3}, \tag{28}$$

where $r_r(\omega)$ is defined in equation (7). In the steady state the eclipse duration would scale as $\nu^{-1/3}$.

The structure of the steady state magnetosphere for an arbitrary power-law spectrum of incident radio radiation is described by equations (B1) and (B2) in Appendix B. With typical parameters for PSR J0737−3039 and $\delta = 2$ we obtain

$$\gamma(r) \approx 1.4 \chi^{-24/55} \left(\frac{r/R_\star}{10^3}\right)^{36/11} B_{\star 12}^{-12/11}, \tag{29}$$

$$\lambda(r) \approx 10^2 \chi^{3/11} \left(\frac{r/R_\star}{10^3}\right)^{49/11} B_{\star 12}^{-20/11}. \tag{30}$$

Absorption by the extra plasma of pulsar A's radio radiation reduces the efficiency of particle heating, thus lowering the value of γ. The dispersion measure variation during the eclipse caused by extra plasma within the steady state magnetosphere is at least 2 orders of magnitude below the current upper bound of 0.016 pc cm^{-3} (Kaspi et al. 2004).

The important distinction of the steady state model is that it *predicts* λ. This determines the lower and upper frequencies between which synchrotron absorption is effective at a given r:

$$\frac{\omega_B}{2\pi}\gamma^{-1} \approx 2\ \mathrm{GHz}\ \chi^{24/55} \left(\frac{r/R_\star}{10^3}\right)^{-69/11} B_{\star 12}^{23/11},$$

$$\frac{\omega_B}{2\pi}\gamma^{2} \approx 5.6\ \mathrm{GHz}\ \chi^{-48/55} \left(\frac{r/R_\star}{10^3}\right)^{39/11} B_{\star 12}^{-13/11}. \tag{31}$$

It follows that the maximum optical depth at frequency ν, an observable quantity, is given by

$$\tau_{\max}(\nu) \approx 3.2 \chi^{15/23} \nu_9^{-20/23}. \tag{32}$$

Figure 1 depicts the evolution of the spectrum of A's radio beam with depth in B's magnetosphere. Power at low frequencies is gradually eaten out by synchrotron absorption as the beam propagates deeper into B's magnetosphere.

Illumination of B's magnetosphere by A's radio beam probably starts only a short time prior to eclipse, so we may be witnessing radio beam attenuation by *dynamically evolving* plasma in B's magnetosphere. The timescale for cold particles to become transrelativistic via cyclotron absorption evaluated from equation (12) is rather short, typically $\lesssim$10 s. Energies of relativistic particles rise exponentially via synchrotron absorption on the timescale

$$t_{\mathrm{heat}}^s \approx 0.78 \left[\frac{e^2}{m_e^2 c^3} F_\omega(\omega_B)\right]^{-1} \approx 320\ \mathrm{s} \left(\frac{r/R_\star}{10^3}\right)^{-6}, \tag{33}$$

so long as the radio spectrum of pulsar A remains unattenuated. Heating has an exponential character for $\delta = 2$ because as γ grows, particles can absorb the incoming radio photons at lower frequencies because ω_B/γ decreases, making more energy from the unabsorbed spectrum available to heat them. This partly compensates for the decrease of the absorption cross section with increasing γ (see eq. [13]). Once γ grows so large that $\tau_\omega(\omega_B/\gamma, r)$ becomes comparable to unity, heating is less efficient and $t_{\mathrm{heat}} \propto \gamma^{8/3}$. We estimate that particles reach $\gamma \sim 10^2$ at $r \approx 10^9$ cm on a timescale of $\sim$5 minutes. This is comparable to estimates of several tens of minutes for the duration of the illumination period judged from the orientation of pulsar A's spin and dipole axes suggested by Demorest et al. (2004). Not much can be said about the timescale needed for the particle density to reach its steady state value. Presumably, this is largely controlled by the rate at which the source near pulsar B is able to supply fresh transrelativistic particles since these are readily trapped.

6. REPROCESSED RADIATION

Energy absorbed by particles in pulsar B's magnetosphere from pulsar A's radio beam is reemitted as synchrotron radiation, albeit with some time delay. Absorption takes place at $\omega \sim \omega_1$ (see eq. [17]), close to the minimum possible frequency, ω_B/γ, and is reemitted at the considerably higher frequency $\omega \sim \gamma^2 \omega_B$. This reemitted radiation, although unimportant locally, may dominate the primary radiation from pulsar A deeper in pulsar B's magnetosphere.

Here we attempt to calculate the properties of the reprocessed radiation for the steady state magnetosphere by applying results from § 5. This requires choosing a low-frequency cutoff, $\nu_{\rm min}$, for the assumed power-law spectrum of A's radio emission. Because there is little evidence for low-frequency cutoffs in the spectra of millisecond pulsars above 100 MHz (Kuzmin & Losovsky 2001), we normalize $\nu_{\rm min}$ to this frequency. From equation (28) we deduce that the energy carried by photons with $\nu \sim \nu_{\rm min}$ is absorbed at a distance $r_{\rm max} \approx 3500 R_\star \nu_{\rm min,8}^{-1/3}$ from pulsar B and reemitted at frequency $\nu_{\rm max} \approx \gamma^2(r_{\rm max})\omega_B(r_{\rm max})/2\pi \approx 360\nu_{\rm min,8}^{-13/11}$ GHz. The latter represents the upper cutoff frequency of the reprocessed radiation because $\gamma^2\omega_B$ increases with increasing r (see eq. [29]). A detailed calculation shows that the radiation reemitted by all the relativistic particles within $r_{\rm max}$ has a flat power-law spectrum F_ν with index close to zero. The local flux of reprocessed photons at $\nu_{\rm max}$ can be estimated from $F_\nu(\nu_{\rm max})\nu_{\rm max} \sim F_\nu(\nu_{\rm min})\nu_{\rm min}$, yielding $F_\nu(\nu_{\rm max}) \sim 2\times10^{-9}$ ergs cm^{-2} s^{-1} Hz^{-1} for a primary spectrum with $\delta = 2$ and time-averaged intensity (at B's location) of $F_\nu(1.4\ {\rm GHz}) = 6\times10^{-6}$ ergs cm^{-2} s^{-1} Hz^{-1}. The reprocessed spectrum intersects the primary radio spectrum of pulsar A at ∼50 GHz, and at frequencies higher than that one has to solve the radiation transfer problem to determine particle heating. Luckily, this is far enough from the GHz region of the spectrum where eclipse observations are usually taken, so we need not worry about such complications. Unfortunately, because of the small covering fraction of B's magnetosphere as seen from A, the flux of reprocessed radiation is too weak to be detected.

7. DISCUSSION

A simple dynamical picture of pulsar A's eclipse by pulsar B's magnetosphere emerges from our considerations. Prior to the onset of illumination by A's radio beam, the number density in the corotating part of B's magnetosphere is equal to $n_{\rm GJ}$. When A's radio beam strikes the magnetosphere of pulsar B, perhaps ∼10 minutes prior to B's inferior conjunction, particles initially present in the magnetosphere rapidly (in ≲10 s) become relativistic. Their energies continue to rise until either synchrotron absorption is balanced by synchrotron emission or illumination by A's radio beam ceases. At the same time neutral plasma accumulates in the magnetosphere as the result of the trapping of particles that stream out in cold beams from a source near B. It is unclear whether the magnetosphere reaches a steady state prior to the eclipse or whether it is still evolving. In either case, a density enhancement $\lambda \sim 200$–300 would be required to match the observed depth and duration of the eclipse. After the illumination of B's magnetosphere by A's radio beam ceases, the particles cool on a typical timescale $t_{\rm cool} \sim 10^2$–10^3 s given by equation (21). As a result, particles no longer mirror, and all plasma beyond that needed to maintain the corotation electric field is lost. This entire cycle repeats each orbital period.

We speculate that part of the asymmetry between eclipse ingress and egress reflects a rise in plasma density in B's magnetosphere during the ∼30 s the eclipse lasts. The optical depth, τ_ω is very sensitive to increasing λ. Not only is τ_ω directly proportional to the total column density of absorbing particles, but it is also proportional to the absorption cross section per particle, which varies as $\gamma^{-5/3}$ and γ decreases with increasing λ. Thus, if λ were growing on a timescale of minutes during eclipse, egress would be deeper than ingress and the eclipse centroid would occur slightly after B reached inferior conjunction, since r_e grows as λ increases (see eq. [20]). In this picture the smooth ingress may partly be caused by the time-variable optical depth at a fixed location rather than the τ_ω variation as the radio beam samples smaller values of r. On the contrary, during egress the optical depth is higher, and the abrupt termination of eclipse may signal the emergence of the radio beam from behind an almost opaque screen. This explanation requires proper timing.

Our model predicts a variation of the polarization of A's radio emission during the course of the eclipse. The polarization signal should be strongly correlated with B's rotational phase in a manner similar to the eclipse light-curve variations found by McLaughlin et al. (2004b). This prediction stems from the fact that synchrotron absorption of photons in different polarization states is sensitive to the angle between the photon $\boldsymbol{k}$-vector and the direction of the magnetic field. Modeling the polarization signature would be facilitated because B's magnetic field should be nearly dipolar at r_e since $R_\star \ll r_e \ll r_{\rm so}$.

Effects of general relativity are very important in PSR J0737−3039. Lai & Rafikov (2005) have demonstrated that gravitational light bending can significantly (by ∼30%) change the minimum-impact parameter at which A's radio beam passes B. Thus, gravitational lensing must play a significant role in shaping the eclipse profile. Moreover, because of the binary's finite orbital eccentricity, $e \approx 0.088$, periastron precession driven mainly by the effects of general relativity forces a 21 yr periodic variation, from $a|\cos i|(1-e)$ to $a|\cos i|(1+e)$, neglecting lensing effects, of the pulsars' minimum projected separation on the plane of the sky (Burgay et al. 2003). By changing the minimum-impact parameter of A's radio beam with respect to B, this should produce observable eclipse profile variations.

Lyutikov (2004) and Arons et al. (2005) have suggested that the eclipse of A's radio beam is caused by synchrotron absorption in the magnetosheath that forms when A's relativistic wind impacts B's magnetosphere. Detailed polarization observations offer a means to distinguish this viable alternative from our model.

The model we have presented is necessarily rather simplistic—it is one-dimensional, it assumes that particle distribution functions are isotropic, and so on. If possible, future work should relax these constraints. A quantitative description of the particle source giving rise to the plasma density enhancement might also be pursued. Further observations have the opportunity to reveal additional clues to properties in the eclipse region. Knowledge of A's radio spectrum is crucial for calculating particle energies, trapping efficiencies, and the eclipse duration. Time-resolved polarization of A's radio emission during eclipse would constrain the magnetic field geometry and particle distribution anisotropy.

Clarifying details of this remarkable example of nonlinear coupling of relativistic plasma to external radiation may provide clues for understanding other puzzling phenomena, such as the modulation of pulsar B's radio emission by radiation from pulsar A (McLaughlin et al. 2004a) and the periodic variations of the pulsar B's brightness that correlate with its orbital phase (Ransom et al. 2005).

We thank Jonathan Arons, Anatoly Spitkovsky, and Sterl Phinney for useful discussions and suggestions and an anonymous referee for bringing the paper of Zhang et al. (2004) to our attention. We are especially grateful to Chris Thompson, whose work on PSR J0737−3039 parallels ours in many respects and who has graciously shared with us his results before publication. R. R. R. acknowledges support from the W. M. Keck Foundation and NSF grant PHY-0070928. Research by P. G. was supported through NSF grant AST 00-98301.

APPENDIX A

PARTICLE ENERGY

To properly compute the heating of particles by synchrotron absorption we evaluate

$$\dot{E}^s_+(r) = \frac{1}{2}\int_{\omega_B/\gamma}^{\infty} F_\omega(\omega, r)\sigma_s(\omega)\, d\omega \approx \frac{4\pi^2}{3^{4/3}\Gamma(1/3)}\frac{F_0 e}{B}\int_0^{\infty}\left(\frac{\omega_B}{\gamma\omega}\right)^{5/3}\left(\frac{\omega_0}{\omega}\right)^{\delta} e^{-\tau_\omega(\omega,r)}\, d\omega, \tag{A1}$$

where the factor 1/2 roughly accounts for shadowing as pulsar B rotates. The lower limit of integration is extended to zero (instead of ω_B/γ) because we are assuming that $\tau_\omega(\omega_B/\gamma, r) \gg 1$. The largest contribution to the local heating comes from ω such that $\tau_\omega(\omega, r) \sim 1$, which, coupled with the condition that $\omega_B/\gamma < \omega$ and equation (15), ensures that $\tau_\omega(\omega_B/\gamma, r) \gtrsim 1$.

Substituting τ_ω from equation (15) into equation (A1) and calculating the integral over $d\omega$, we find

$$\dot{E}^s_+(r) = \frac{3\pi\zeta_1}{5}\Gamma\left(\frac{2+3\delta}{5}\right)\left[\frac{4\pi}{3^{4/3}\zeta_1\Gamma(1/3)}\right]^{3(1-\delta)/5}\frac{e\omega_B F_0}{B}\left(\frac{\omega_0}{\omega_B}\right)^{\delta}\left[\lambda(r)\frac{\Omega_B r}{c}\right]^{-(2+3\delta)/5}\gamma^{\delta-1}. \tag{A2}$$

Balancing this heating rate by the cooling rate (eq. [10]) yields

$$\gamma(r) = \left[\frac{27\pi\zeta_1}{20}\Gamma\left(\frac{2+3\delta}{5}\right)\left(\frac{4\pi}{3^{4/3}\zeta_1\Gamma(1/3)}\right)^{[3(1-\delta)]/5}\right]^{1/(3-\delta)}\left[\frac{F_0}{m_e\omega_B^2}\left(\frac{\omega_0}{\omega_B}\right)^{\delta}\right]^{1/(3-\delta)}\left[\lambda(r)\frac{\Omega_B r}{c}\right]^{-[2+3\delta]/[5(3-\delta)]}. \tag{A3}$$

Substituting equation (A3) into equation (15), assuming $\tau_\omega(\omega) = 1$, and solving for r_e, we obtain the size of eclipsing region at frequency ω:

$$r_e(\omega) = R_\star\left[\frac{4\pi}{3^{4/3}\Gamma(1/3)\zeta_1}\right]^{3/32}\left[\frac{20}{27\pi\zeta_1\Gamma((2+3\delta)/5)}\right]^{5/64}\left(\frac{\omega_{B\star}}{\omega}\right)^{[5(3-\delta)]/64}\left[\frac{F_0}{m_e\omega_{B\star}^2}\left(\frac{\omega_0}{\omega_{B\star}}\right)^{\delta}\right]^{-5/64}\left(\lambda(r_e)\frac{\Omega_B R_\star}{c}\right)^{11/64}. \tag{A4}$$

The constant coefficients in these expressions depend on the values of the parameters δ and ζ_1. For the radio spectrum of pulsar A with $\delta = 2$ and λ independent of r, it follows that $\zeta_1 = 64/3$. Then the coefficient in equation (A3) is $\approx$481.

APPENDIX B

STEADILY ILLUMINATED MAGNETOSPHERE

By combining equations (15), (27), and (A3), γ is self-consistently determined to be

$$\gamma(r) = \left[\frac{9\pi^2}{3^{1/3}5}\frac{\Gamma((2+3\delta)/5)}{\Gamma(1/3)}\chi^{-(2+3\delta)/5}\frac{F_0}{m_e\omega_B^2}\left(\frac{\omega_0}{\omega_B}\right)^{\delta}\right]^{3/11}. \tag{B1}$$

From equations (15), (27), and (B1), we find that

$$\lambda(r) = \frac{3^{4/3}5\Gamma(1/3)}{4\pi}\left[\frac{9\pi^2}{3^{1/3}5}\frac{\Gamma((2+3\delta)/5)}{\Gamma(1/3)}\right]^{5/11}\chi^{3(3-\delta)/11}\frac{c}{\Omega_B r}\left[\frac{F_0}{m_e\omega_B^2}\left(\frac{\omega_0}{\omega_B}\right)^{\delta}\right]^{5/11}. \tag{B2}$$

Equations (B1) and (B2) imply that $\zeta_1 = 5$; see equation (17). These formulae determine the structure of the steady state magnetosphere for arbitrary $\delta > 1$.

REFERENCES

Arons, J., Backer, D. C., Spitkovsky, A., & Kaspi, V. 2005, in ASP Conf. Ser. 328, Binary Radio Pulsars, ed. F. A. Rasio & I. H. Stairs (San Francisco: ASP), 95

Blandford, R. D., & Scharlemann, E. T. 1976, MNRAS, 174, 59

Burgay, M., et al. 2003, Nature, 426, 531

Canuto, V., Lodenquai, J., & Ruderman, M. 1971, Phys. Rev. D, 3, 2303

Cheng, K. S., Ho, C., & Ruderman, M. 1986a, ApJ, 300, 500

———. 1986b, ApJ, 300, 522

Coles, W. A., McLaughlin, M. A., Rickett, B. J., Lyne, A. G., & Bhat, N. D. R. 2005, ApJ, 623, 392

Daugherty, J. K., & Ventura, J. 1978, Phys. Rev. D, 3, 2303

Demorest, P., Ramachandran, R., Backer, D. C., Ransom, S. M., Kaspi, V., Arons, J., & Spitkovsky, A. 2004, ApJ, 615, L137

Goldreich, P., & Julian, W. H. 1969, ApJ, 157, 869

Kaspi, V., Ransom, S. M., Backer, D. C., Ramachandran, R., Demorest, P., Arons, J., & Spitkovsky, A. 2004, ApJ, 613, L137

Kuzmin, A. D., & Losovsky B. Y. 2001, A&A, 368, 230

Lai, D., & Rafikov, R. R. 2005, ApJ, 621, L41

Lyne, A. G., et al. 2004, Science, 303, 1153

Lyubarskii, Y. E., & Petrova, S. A. 1998, A&A, 337, 433

Lyutikov, M. 2004, MNRAS, 353, 1095

Lyutikov, M., & Thompson, C. 2005, ApJ, in press

McLaughlin, M. A., et al. 2004a, ApJ, 613, L57

———. 2004b, ApJ, 616, L131

Mikhailovskii, A. B., Onishchenko, O. G., Suramlishvili, G. I., & Sharapov, S. E. 1982, Sov. Astron. Lett., 8, 369

Ransom, S. M., Demorest, P., Kaspi, V., Ramachandran, R., & Backer, D. C. 2005, in ASP Conf. Ser. 328, Binary Radio Pulsars, ed. F. A. Rasio & I. H. Stairs (San Francisco: ASP), 73

Rybicki, G. B., & Lightman, A. P. 1979, Radiative Processes in Astrophysics (New York: Wiley)

Wang, F. Y.-H., Ruderman, M., Halpern, J. P., & Zhu, T. 1998, ApJ, 498, 373

Zhang, L., Cheng, K. S., Jiang, Z. J., & Leung, P. 2004, ApJ, 604, 317